Low-energy electron-impact excitation of the $^{3,1}A_2(n \rightarrow \pi^*)$ states of formaldehyde

Qiyan Sun, Carl Winstead, and Vincent McKoy
A. A. Noyes Laboratory of Chemical Physics, California Institute of Technology, Pasadena, California 91125

José S. E. Germano
Instituto Técnico da Aeronautica, Centro Técnico Aeroespacial, 12200 São José dos Campos, São Paulo, Brazil

Marco A. P. Lima
Instituto de Física Gleb Wataghin and Departmento de Electrônica Quântica, Universidade Estadual de Campinas, 13081 Campinas, São Paulo, Brazil

(Received 5 March 1992)

A three-state calculation of electron-impact excitation of formaldehyde to the $\tilde{a}\,^3A_2$ and $\tilde{A}\,^1A_2$ states is carried out using the Schwinger multichannel variational method. The integral and differential cross sections so obtained agree fairly well with theoretical results obtained using the complex Kohn method. Though agreement between the calculated integral cross section and the single available experimental measurement is qualitative, similar conclusions regarding the excitation mechanism are reached. A generalization of the selection rule for $(\Sigma^+ \leftrightarrow \Sigma^-)$ electron-impact excitation of diatomic molecules is used to explain the shape of the differential cross sections for the $\tilde{a}\,^3A_2$ and $\tilde{A}\,^1A_2$ excitations.

PACS number(s): 34.80.Gs

I. INTRODUCTION

The Schwinger multichannel (SMC) variational method [1] has been developed into a useful tool for theoretical studies of low-energy electron-molecule scattering and has been applied to various electron-molecule collision problems over the past several years [2]. The SMC method is a multichannel extension of the Schwinger variational principle [3], which preserves several important aspects of that principle while possessing features desirable for electron-molecule scattering. For example, as in the original Schwinger principle, the trial scattering wave function can be expanded in a purely L^2 basis. Furthermore, if a set of Cartesian Gaussian functions is chosen as the basis for the entire calculation, all matrix elements arising in the variational expression except those associated with the Green's function can be evaluated analytically for a molecule of arbitrary geometry. The SMC method has also been improved recently in two major respects. One is the use of a numerical quadrature scheme for evaluating the matrix elements involving the projected Green's function [4], thereby avoiding the requirement of large basis sets and possible errors from the insertion techniques used previously [1,5]. The other improvement is implementation of the code on distributed-memory massively parallel computers [6]. These developments and the rapid growth in power of parallel computers have facilitated the study of a number of elastic and inelastic electron–polyatomic-molecule collision problems. The results of some earlier studies have been reported in recent publications [6,7]. In the present work, we report the results of three-channel calculations of electron-impact excitation of the $\tilde{a}\,^3A_2$ and $\tilde{A}\,^1A_2$ states of formaldehyde.

As a prototype carbonyl molecule, formaldehyde has been the subject of numerous optical experiments and molecular structure calculations. These have been reviewed by Moule and Walsh [8]. However, relatively few electron-impact studies of H_2CO have been carried out. Experimental studies of elastic and vibrationally inelastic electron scattering sought to characterize the low-energy shape resonance around 1 eV [9]. Several studies of electron-impact excitation of formaldehyde aimed at locating and characterizing the low-lying electronic bands [10–12]. Chutjian measured relative differential cross sections for several electronic transitions in a crossed-beam-type experiment [11], and van Veen, van Dijk, and Brongersma measured an excitation function for the $(n \rightarrow \pi^*)$ transition using the trapped-electron method [12]. On the theoretical side, the complex Kohn method has recently been used to study the low-energy shape resonance [13] and electron-impact excitation of the $^{1,3}A_2$ states of formaldehyde [14].

The present study is part of ongoing research that aims to produce cross-section information for various low-energy electron–polyatomic-molecule collision processes using the SMC method on distributed-memory parallel computers, with an emphasis on data that may be useful in modeling low-temperature collisional plasmas [15]. Formaldehyde is of interest in part because there are other theoretical and experimental results, although limited, available for comparison. The present work also serves as a prelude to further studies of carbonyl molecules, such as acetaldehyde and acetone, and of other organic molecules generally.

In the next section the SMC method is briefly summarized. In Sec. III the numerical procedures are described. The results and discussion are presented in Sec. IV, and a summary and conclusions are given in Sec. V.

II. THEORETICAL METHOD

The details of the SMC method and its current implementation have been given before [1,4,6]. For convenience we recall some key equations here.

The total Hamiltonian for a scattering electron colliding with an N-electron molecule can be written as

$$H=(H_N+T_{N+1})+V=H_0+V\ , \tag{1}$$

where H_N is the Hamiltonian of the molecule, T_{N+1} is the kinetic-energy operator of the scattering electron, and V is the interaction potential between the scattering electron and the molecule. It can be shown that the full scattering wave function satisfies [1]

$$P\Psi_\Gamma^{(+)}=S_{\mathbf{k}_\Gamma}+G_P^{(+)}V\Psi_\Gamma^{(+)} \tag{2}$$

and the following inhomogeneous equation:

$$A^{(+)}\Psi_\Gamma^{(+)}=VS_{\mathbf{k}_\Gamma}\ , \tag{3}$$

where Γ is a channel label, $S_{\mathbf{k}_\Gamma}=\chi_\Gamma\exp(i\mathbf{k}_\Gamma\cdot\mathbf{r}_{N+1})$ are eigenfunctions of H_0, and

$$A^{(+)}=\tfrac{1}{2}(PV+VP)-VG_P^{(+)}V+\frac{1}{N+1}\left[\hat{H}-\frac{N+1}{2}(\hat{H}P+P\hat{H})\right]\ , \tag{4}$$

where $\hat{H}=E-H$, P is a projection operator onto the open-channel space χ_Γ of H_N, and $G_P^{(+)}$ is the projected outgoing-wave Green's function.

Based on Eqs. (2) and (3), a variational functional for the scattering amplitude in the linear momentum representation can be constructed

$$f(\mathbf{k}_{\Gamma'},\mathbf{k}_\Gamma)=-\frac{1}{2\pi}(\langle S_{\mathbf{k}_{\Gamma'}}|V|\Psi_\Gamma^{(+)}\rangle+\langle\Psi_{\Gamma'}^{(-)}|V|S_{\mathbf{k}_\Gamma}\rangle-\langle\Psi_{\Gamma'}^{(-)}|A^{(+)}|\Psi_\Gamma^{(+)}\rangle)\ . \tag{5}$$

The trial scattering wave functions used in Eq. (5) need not satisfy scattering boundary conditions and can be expanded in $(N+1)$-electron Slater determinants Φ_m:

$$\Psi^{(\pm)}=\sum_m a_m^{(\pm)}\Phi_m\ . \tag{6}$$

The stationary value of Eq. (5) gives our working equation for the scattering amplitude,

$$f(\mathbf{k}_{\Gamma'},\mathbf{k}_\Gamma)=-\frac{1}{2\pi}\sum_{m,n}\langle S_{\mathbf{k}_{\Gamma'}}|V|\Phi_m\rangle(d^{-1})_{mn}\langle\Phi_n|V|S_{\mathbf{k}_\Gamma}\rangle, \tag{7}$$

where

$$d_{mn}=\langle\Phi_m|A^{(+)}|\Phi_n\rangle\ . \tag{8}$$

If the Φ_m are expanded in Cartesian Gaussian functions, all the matrix elements in Eq. (7) can be evaluated analytically except those involving the projected Green's function, i.e., $\langle\Phi_m|VG_P^{(+)}V|\Phi_n\rangle$. Evaluation of these elements is the computationally substantial step of our calculation. An "α-insertion" technique [1] and subsequently a "k-insertion" technique [5] were introduced to evaluate those matrix elements; however, both techniques required large Gaussian basis sets to approach mathematical completeness, complicating applications of the SMC method to electron–polyatomic-molecule collisions. Recently, a numerical quadrature technique has been introduced for evaluating those matrix elements [4]. This approach avoids the requirement of large basis sets and allows a more reliable assessment of convergence than is possible with insertion techniques.

The integral cross sections are given by

$$\sigma^F(k_{\Gamma'},k_\Gamma)=\frac{k_{\Gamma'}}{k_\Gamma}\int\int|f(\mathbf{k}_{\Gamma'},\mathbf{k}_\Gamma)|^2d\hat{\mathbf{k}}_{\Gamma'}d\hat{\mathbf{k}}_\Gamma\ , \tag{9}$$

where $\hat{\mathbf{k}}_{\Gamma'(\Gamma)}$ are directions of the outgoing (incoming) plane waves. Transformation of the scattering amplitude from the linear momentum representation to the angular momentum representation leads to the partial-wave amplitude in the body-fixed frame,

$$f_{lm}^{l'm'}(k_{\Gamma'},k_\Gamma)=\int\int Y_{l'm'}^*(\hat{\mathbf{k}}_{\Gamma'})f(\hat{\mathbf{k}}_{\Gamma'},\mathbf{k}_\Gamma)Y_{lm}(\hat{\mathbf{k}}_\Gamma)d\hat{\mathbf{k}}_{\Gamma'}d\hat{\mathbf{k}}_\Gamma\ , \tag{10}$$

where Y_{lm} are spherical harmonics. Based on Eq. (10), the partial-wave differential and integral cross sections are given by

$$\sigma_{lm}^{l'm'}(k_{\Gamma'},k_\Gamma)=\frac{k_{\Gamma'}}{k_\Gamma}|f_{lm}^{l'm'}(k_{\Gamma'},k_\Gamma)|^2 \tag{11}$$

and

$$\sigma^P(k_{\Gamma'},k_\Gamma)=\sum_{l=0}^{l_{\max}}\sum_{m=-l}^{l}\sum_{l'=0}^{l_{\max}}\sum_{m'=-l'}^{l'}\sigma_{lm}^{l'm'}(k_{\Gamma'},k_\Gamma)\ . \tag{12}$$

The differential cross sections are obtained by transforming the partial-wave amplitude in Eq. (10) from body frame to laboratory frame and then averaging over the Euler angles. The procedure is straightforward and details are given elsewhere [16].

III. CALCULATIONS

In this study we described the target states by single-configuration wave functions. The ground-state wave function was obtained at the self-consistent-field (SCF) level using Dunning's [17] $(4s)/[3s]$ basis set for hydrogen and $(9s5p)/[5s3p]$ sets for carbon and oxygen, augmented by one polarization d function on carbon and one on oxygen, with exponents of 0.75 and 0.85, respectively. Using this basis, the ground-state SCF energy at the experimental nuclear geometry was -113.894 a.u., compared to the near-Hartree-Fock limit value of -113.902 a.u. [18]. The ground-state dipole moment was 2.792 D; the corresponding experimental value is 2.33 D [19]. Wave functions for the $\tilde{a}\,^3A_2$ and $\tilde{A}\,^1A_2$ excited states were obtained using the improved-virtual-orbital (IVO) approach [20] in the same basis set and at the same geometry. The vertical excitation energies were 4.077 eV for the triplet state and 4.801 eV for the singlet state. The corresponding experimental values are 3.45 and 4.26 eV, respectively [11]. We have also calculated dipole mo-

TABLE I. Exponents of additional Cartesian Gaussian functions used in the scattering calculation.

Center	Type	Exponents
Carbon	s	1.7, 0.3
	p_y	0.7, 0.2
	p_x, p_z	0.2
	d_{xy}, d_{yz}	1.5, 0.375
	d_{xz}	1, 0.5, 0.3, 0.15
Oxygen	s	2.8, 0.5
	p_y	1.4, 0.45
	p_x, p_z	0.45
	d_{xy}, d_{yz}	1.7, 0.425
	d_{xz}	1.2, 0.6, 0.35, 0.2
Center of mass	s	0.1, 0.05, 0.02
	p_y	0.1, 0.03, 0.01
	p_x, p_z	0.5, 0.1, 0.03, 0.01
	d_{xy}, d_{yz}	0.3, 0.1, 0.03, 0.01
	d_{xz}	0.3, 0.1, 0.05

ments for the excited states, obtaining 1.32 D for the $^3A_2$ state and 1.29 D for the $^1A_2$ state. Experimental values are 1.29±0.03 D [21] and 1.56±0.07 D [22] for the $^3A_2$ state and the $^1A_2$ state, respectively. In the scattering calculations, the π^* IVO of the $^3A_2$ state was used to construct both target singlet and triplet excited states, but the $^1A_2$ threshold was taken from the singlet IVO calculation.

To describe the scattering wave functions, we employed the virtual orbitals from the target-state calculations described above, together with additional Gaussian functions, given in Table I. In interpreting the table, it should be noted that the molecule was chosen to lie in the xy plane, with the C—O bond along the y axis. For computational convenience, these additional functions are Schmidt orthogonalized to the orbitals of the target basis and to each other. Proper correlation terms [23] were included in the calculation in order to relax these strong-orthogonality constraints.

Several quadrature schemes were tested in evaluating the matrix elements involving the projected Green's function and the integral cross sections in Eq. (9). We believe the final quadrature schemes used gave negligible errors in all calculations.

In the present study, we found that it was important to monitor the condition number of the matrix d_{mn} when solving the system of linear equations associated with Eq. (7). Numerical techniques previously described [24], based on singular-value decomposition, were used to eliminate instabilities associated with poor conditioning. Extensive calculations in a wide range of basis sets indicate that the results presented below are well converged to the appropriate three-channel limit.

IV. RESULTS AND DISCUSSION

The inelastic integral cross sections for the $\tilde{X}\,^1A_1 \rightarrow \tilde{a}\,^3A_2$ and $\tilde{X}\,^1A_1 \rightarrow \tilde{A}\,^1A_2$ transitions are shown in Fig. 1. Four sets of cross-section data have been plotted. Two are the present results as calculated from Eq.

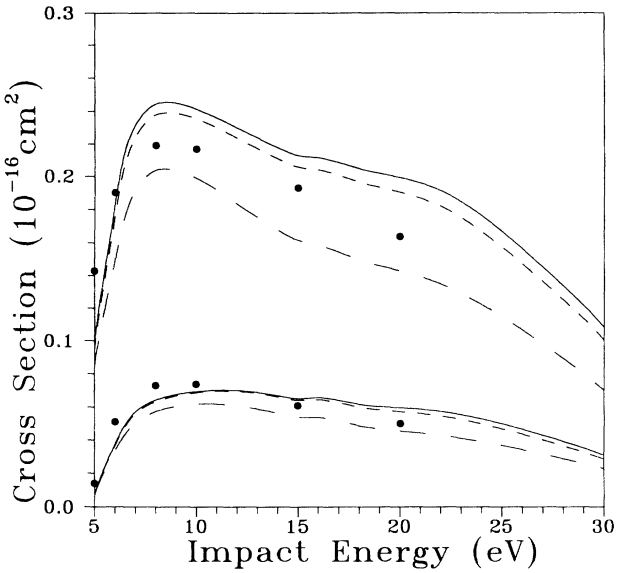

FIG. 1. Integral cross sections for the $\tilde{X}\,^1A_1 \rightarrow \tilde{a}\,^3A_2$ (upper four sets of data) and $\tilde{X}\,^1A_1 \rightarrow \tilde{A}\,^1A_2$ (lower four sets) electronic excitations of formaldehyde. The solid curves are the present results; the short-dashed and long-dashed curves are the present results truncated at $l_{max}=7$ and $l_{max}=4$, respectively; the solid circles are complex-Kohn results of Rescigno, Lengsfield, and McCurdy (Ref. [14]).

(12), with the maximum angular momentum in both incoming and outgoing channels limited respectively to $l_{max}=7$ and $l_{max}=4$, and one is the present result as obtained from Eq. (9). The remaining set is the calculation of Rescigno, Lengsfield, and McCurdy using the complex Kohn method [14]. We note that the full integral cross section from Eq. (9), which includes contributions from high partial waves, differs only slightly from that obtained with $l_{max}=7$; the latter is presented in the figure in order to be consistent with the differential cross sections given below.

Both the $\tilde{A}\,^1A_2$ and the $\tilde{a}\,^3A_2$ excitations are unfavored on symmetry grounds to be discussed below, and the excitation cross sections are quite small in comparison to typical valence excitation cross sections. As seen from Fig. 1, the singlet and triplet cross sections are of similar form and are rather featureless, and the ratio of the triplet to the singlet cross section at most energies is close to the 3:1 value that would be expected from degeneracy alone, suggesting similar excitation mechanisms for each channel.

The present results are in fair agreement with those of Rescigno, Lengsfield, and McCurdy; moreover, truncating our results at $l_{max}=4$ in order to make them directly comparable to those of Ref. [14] improves the agreement for the triplet excitation, though not for the singlet. Some of the remaining discrepancies may be due to the use of different target wave functions. Rescigno, Lengsfield, and McCurdy constructed their excited-state functions by orthogonalizing the π^* orbital from an excited-state SCF calculation to the occupied b_1 orbital from the SCF ground state [14], while the IVO approach

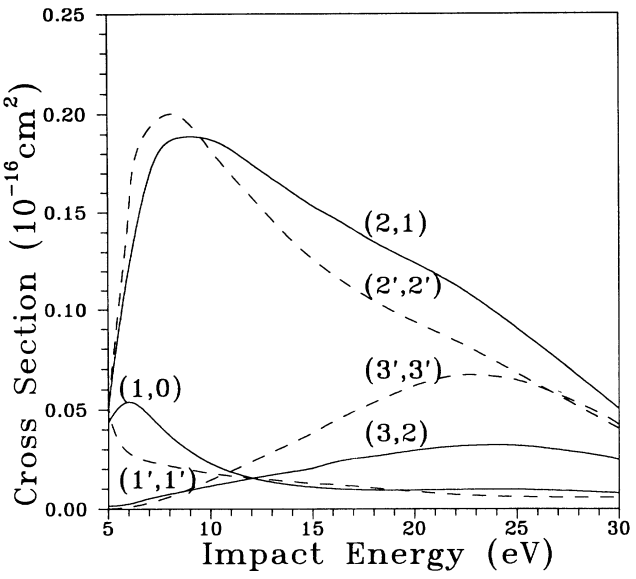

FIG. 2. Principal partial-wave contributions (l,m) in the entrance channel (solid curves) and (l',m') in the exit channel (dashed curves) to the $\tilde{a}\,^3A_2$ excitation cross section of Fig. 1. The azimuthal quantum numbers m and m' refer to a z axis perpendicular to the molecular plane.

was employed in the present work. Small differences in the excited-state energies indicate that the two approaches do in fact give somewhat different π^* orbitals.

To analyze the dynamics, a partial-wave decomposition of the inelastic cross sections was done. The dominant contributions are shown in Fig. 2 for the triplet excitation and in Fig. 3 for the singlet excitation. The solid curves in Figs. 2 and 3 were obtained by holding the incoming partial wave (l,m) fixed and summing over all outgoing waves (l',m'); conversely, the dashed curves are obtained by summing over all (l,m) for fixed values of l' and m'. Note that m quantum numbers here refer to the projection of l on an axis perpendicular to the molecular plane due to the axis system used in the calculation. For both the singlet and the triplet channels, the main contributions are seen to be $(l,m)=(2,1)$ in the entrance channel and $(l',m')=(2,2)$ in the exit channel. This exit-channel symmetry is not consistent with the presence of a $(\pi^*)^2$ core-excited shape resonance of the type proposed by van Veen, van Dijk, and Brongersma [12]; moreover, as Figs. 2 and 3 show, the (2,2) peak is very broad, and may more probably be ascribed to nonresonant excitation.

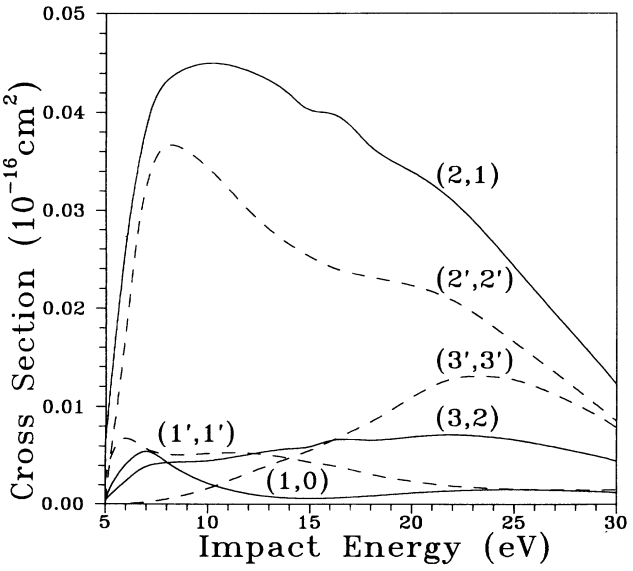

FIG. 3. As in Fig. 2, for the $\tilde{A}\,^1A_2$ state.

The differential cross sections at selected energies are shown in Figs. 4 and 5, along with the results of Rescigno, Lengsfield, and McCurdy [14]. On the whole, there is quite good agreement on the shape of the differential cross sections, though some differences in detail are evident. The relative magnitudes of course reflect the differences in the integral cross sections that were seen in Fig. 1, with substantial differences in the immediate vicinity of threshold [Figs. 4(a) and 4(b)] and fairly good agreement at higher energies.

The differential cross sections show minima at scattering angles of 0° and 180°. This behavior is common to a class of transitions. To understand the mechanism, consider a molecule with a reflection plane that undergoes a transition between two states having opposite signs under this reflection. If the electron's direction of incidence lies in this symmetry plane for scattering at 0° or 180°, so must its direction of departure. The overall wave function for target plus scatterer therefore has the same reflection symmetry as the wave function for the target itself, and a transition between the two states would thus

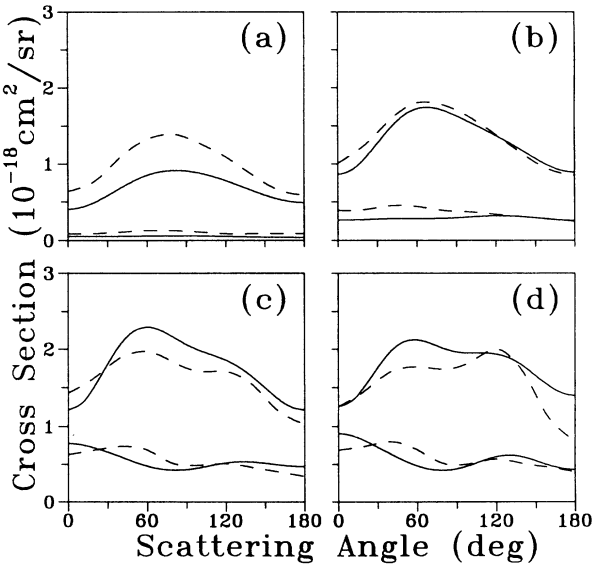

FIG. 4. Differential cross sections for the $\tilde{X}\,^1A_1 \rightarrow \tilde{a}\,^3A_2$ (upper two curves) and $\tilde{X}\,^1A_1 \rightarrow \tilde{A}\,^1A_2$ (lower two curves) electronic excitations of formaldehyde, shown at impact energies of (a) 5, (b) 6, (c) 8, and (d) 10 eV. The solid curves are the present results with $l_{max}=7$; the dashed curves are the complex-Kohn results of Rescigno, Lengsfield, and McCurdy, Ref. [14].

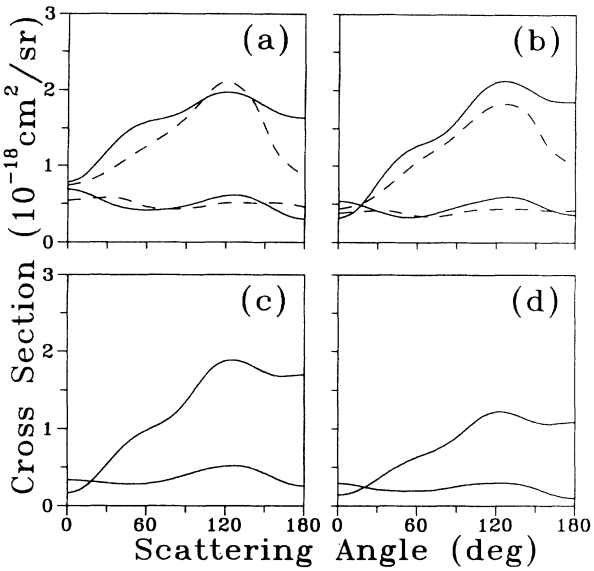

FIG. 5. As in Fig. 4, at (a) 15, (b) 20, (c) 25, and (d) 30 eV, except no complex-Kohn results at 25 or 30 eV.

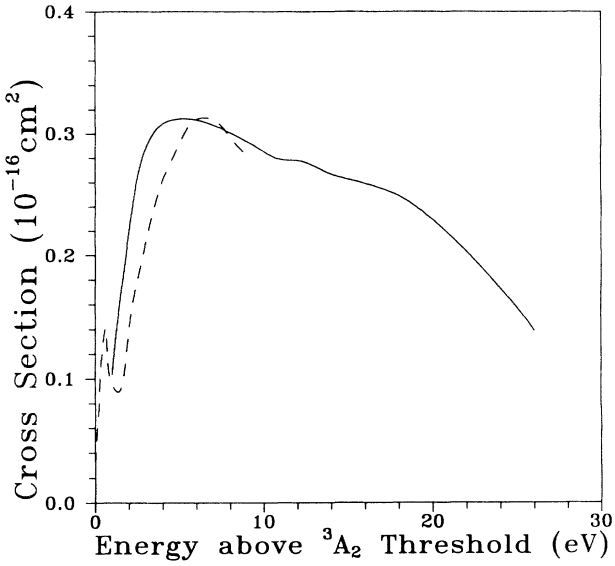

FIG. 6. Sum of integral cross sections for the $\tilde{X}\,^1A_1 \rightarrow \tilde{a}\,^3A_2$ and $\tilde{X}\,^1A_1 \rightarrow \tilde{A}\,^1A_2$ electronic excitations of formaldehyde. The solid line is the present theoretical result; the dashed line is the experimental result of Ref. [12], normalized to the calculation of 6 eV.

violate conservation of this symmetry. For a linear molecule, the incident and scattering electron must always lie in a symmetry plane when the cross section is measured at 0° or 180°; thus, if the target wave function changes parity ($\Sigma^+ \leftrightarrow \Sigma^-$) during the scattering, the cross section is exactly zero at 0° and 180° scattering angles, as pointed out originally by Cartwright *et al.* [25].

Now consider formaldehyde. There are two reflection planes containing the C—O bond. The $^1A_1$ ground-state wave function does not change sign under either of these reflections, but the $^{3,1}A_2$ excited-state wave functions change sign under both. Due to the symmetry rules noted above, the differential cross sections are zero at 0° and 180° scattering angles for any direction of incidence lying in either of these planes. One also expects the forward and backward scattering to be weak for directions of incidence near either of these symmetry planes. In view of these factors, even after averaging the cross sections over all orientations, we would expect relatively weak forward and backward scattering. This is just what we have seen for the triplet excitation. The behavior is less marked for the singlet transition; however, even in that case the rather isotropic distribution, which contrasts with the strongly forward-peaked behavior frequently seen in singlet-to-singlet excitation, may reflect the operation of the same mechanism.

It might further be pointed out that a zero cross section is required whenever the directions of incidence and departure lie in the same symmetry plane, and not just for forward and backward scattering, leading to the expectation that the transition should on the whole be weak, as is indeed observed. It should also be remarked that Rescigno, Lengsfield, and McCurdy have presented a related explanation based on the correlation between the states of formaldehyde involved in the present transitions and Σ^+ and Σ^- states of oxygen [14]; here we have attempted to provide more detail as to how this analogy operates in the reduced symmetry of a polyatomic molecule.

The present integral cross section is compared to the measured excitation function of van Veen, van Dijk, and Brongersma [12] in Fig. 6. In the measurement, only relative values are reported, the singlet and triplet excitations are not separated, and the threshold energy used is not clear. For comparison, we summed our singlet and triplet cross sections, measured the electron energy with respect to the triplet threshold, and normalized the experimental excitation function at 6 eV. Fair agreement between the present results and the measurement is seen. Both curves show a quick rise in the threshold region. The measured excitation function comes down quickly above 7 eV, at least partly due to an instrumental effect described by van Veen, van Dijk, and Brongersma [12]. Our results for the individual cross sections (Fig. 1) support the prediction of Ref. [12] that the triplet excitation is dominant in the energy range considered and that the singlet excitation is growing more significant with the increase of electron energy.

The sharp peak near threshold in the measured excitation function was attributed by van Veen, van Dijk, and Brongersma to a core-excited shape resonance with a $n(\pi^*)^2$ configuration. No such structure appears in either the present theoretical calculation or the calculation of Rescigno, Lengsfield, and McCurdy. In fact, we have diagonalized the $(N+1)$-electron Hamiltonian in a Gaussian basis and found that the relevant $n(\pi^*)^2$ configuration lies about 3 eV above the singlet threshold, well above the position of the experimental feature. Moreover, the $(l',m')=(2,2)$ component that dominates the scattering (Figs. 2 and 3) is, as discussed above, of inappropriate symmetry for a $(\pi^*)^2$ resonance and probably arises from nonresonant scattering. On the other hand, target-polarization effects neglected in the present

calculations will tend both to sharpen and to shift to lower energy any core-excited shape resonance that may be present. Further work, both experimental and theoretical, would be useful in order to clarify the situation.

V. SUMMARY AND CONCLUSIONS

We have carried out a three-state calculation of electron-impact excitation of formaldehyde to the $\tilde{a}\,^3A_2$ and $\tilde{A}\,^1A_2$ states using the Schwinger multichannel method. Both integral and differential cross sections have been compared with the theoretical results of Rescigno, Lengsfield, and McCurdy [14], which were obtained using the complex Kohn method. Agreement is in general good. This is an encouraging circumstance, since for the present case it has been possible to compare two *ab initio* methods for calculating electron-impact excitation cross sections of polyatomic molecules. We have further made a comparison between the present integral cross section and the measured excitation function of van Veen, van Dijk, and Brongersma. Though the agreement is qualitative, and in particular the narrow peak observed by van Veen, van Dijk, and Brongersma is absent in the calculation, similar conclusions on the excitation mechanism were reached. In addition, we have discussed how the ($\Sigma^+ \leftrightarrow \Sigma^-$) selection rule for electron scattering from diatomic molecules generalizes to the case of a polyatomic target, and we have used that generalization to explain the striking shape and relatively small magnitude of the differential cross sections for the $\tilde{a}\,^3A_2$ and $\tilde{A}\,^1A_2$ excitations.

ACKNOWLEDGMENTS

This work made use of computer resources provided by the Concurrent Supercomputing Consortium, the Caltech Concurrent Supercomputing Facilities, and the JPL-Caltech Supercomputing Project. Financial support was provided by the National Science Foundation under Grant Nos. PHY-9021933, INT-8714948, and INT-9106425.

[1] K. Takatsuka and V. McKoy, Phys. Rev. A **24**, 2473 (1981); *ibid.* **30**, 1734 (1984).

[2] L. M. Brescansin, M. A. P. Lima, W. M. Huo, and V. McKoy, Phys. Rev. B **32**, 7122 (1985); L. M. Brescansin, M. A. P. Lima, T. L. Gibson, V. McKoy, and W. M. Huo, J. Chem. Phys. **85**, 1854 (1986); M. A. P. Lima, T. L. Gibson, V. McKoy, and W. M. Huo, Phys. Rev. A **38**, 4527 (1988); H. P. Pritchard, M. A. P. Lima, and V. McKoy, *ibid.* **39**, 2392 (1989); M. A. P. Lima, K. Watari, and V. McKoy, *ibid.* **39**, 4312 (1989); H. P. Pritchard, V. McKoy, and M. A. P. Lima, *ibid.* **41**, 546 (1990); C. Winstead and V. McKoy, *ibid.* **42**, 5357 (1990).

[3] J. Schwinger, Phys. Rev. **72**, 742 (1947).

[4] M. A. P. Lima, L. M. Brescansin, A. J. R. da Silva, C. Winstead, and V. McKoy, Phys. Rev. A **41**, 327 (1990).

[5] W. M. Huo, T. L. Gibson, M. A. P. Lima, and V. McKoy, Phys. Rev. A **36**, 1632 (1987); W. M. Huo, M. A. P. Lima, T. L. Gibson, and V. McKoy, *ibid.* **36**, 1642 (1987).

[6] P. G. Hipes, C. Winstead, M. A. P. Lima, and V. McKoy, in *Proceedings of the Fifth Distributed Memory Computing Conference, Vol. I: Applications,* edited by D. W. Walker and Q. F. Stout (IEEE Computer Society, Los Alamitos, CA, 1990), p. 498.

[7] C. Winstead, P. G. Hipes, M. A. P. Lima, and V. McKoy, J. Chem. Phys. **94**, 5455 (1991); Q. Sun, C. Winstead, V. McKoy, and M. A. P. Lima, *ibid.* **96**, 3531 (1992); C. Winstead, Q. Sun, and V. McKoy, *ibid.* **96**, 4246 (1992); C. Winstead, Q. Sun, P. G. Hipes, M. A. P. Lima, and V. McKoy, Aust. J. Phys. (to be published).

[8] D. C. Moule and A. D. Walsh, Chem. Rev. **75**, 67 (1971).

[9] P. D. Burrow and J. A. Michejda, Chem. Phys. Lett. **42**, 223 (1976); C. Benoit and R. Abouaf, *ibid.* **123**, 134 (1986); C. Benoit, R. Abouaf, and S. Cvejanovic, Chem. Phys. **117**, 295 (1987).

[10] M. J. Weiss, C. E. Kuyatt, and S. Mielczarek, J. Chem. Phys. **54**, 4147 (1971); S. Taylor, D. G. Wilden, and J. Comer, Chem. Phys. **70**, 291 (1982); K. N. Walzl, C. F. Koerting, and A. Kuppermann, J. Chem. Phys. **87**, 3796 (1987).

[11] A. Chutjian, J. Chem. Phys. **61**, 4279 (1974).

[12] E. H. van Veen, W. L. van Dijk, and H. H. Brongersma, Chem. Phys. **16**, 337 (1976).

[13] T. N. Rescigno, C. W. McCurdy, and B. I. Schneider, Phys. Rev. Lett. **63**, 248 (1989); B. I. Schneider, T. N. Rescigno, and C. W. McCurdy, Phys. Rev. A **42**, 3132 (1990).

[14] T. N. Rescigno, B. H. Lengsfield III, and C. W. McCurdy, Phys. Rev. A **41**, 2462 (1990).

[15] See, for example, *Plasma Reactions and Their Applications* (ASM International, Metals Park, OH, 1988); and *Plasma Etching: An Introduction,* edited by D. M. Manos and D. L. Flamm (Academic, San Diego, 1989).

[16] M. A. P. Lima, T. L. Gibson, K. Takatsuka, and V. McKoy, Phys. Rev. A **30**, 1741 (1984).

[17] T. H. Dunning, J. Chem. Phys. **53**, 2823 (1970).

[18] P. Pulay, G. Fogarasi, F. Pang, and J. E. Boggs, J. Am. Chem. Soc. **101**, 2550 (1979).

[19] *CRC Handbook of Chemistry and Physics,* edited by R. C. Weast and M. J. Astle, 60th ed. (CRC, Boca Raton, FL, 1980), p. E-63.

[20] W. A. Goddard and W. J. Hunt, Chem. Phys. Lett. **24**, 464 (1974).

[21] A. D. Buckingham, D. A. Ramsay, and J. Tyrrell, Can. J. Phys. **48**, 1242 (1970).

[22] D. E. Freeman and W. Klemperer, J. Chem. Phys. **40**, 604 (1964); **45**, 52 (1966).

[23] M. A. P. Lima, T. L. Gibson, W. M. Huo, and V. McKoy, J. Phys. B **18**, L865 (1985).

[24] C. Winstead and V. McKoy, Phys. Rev. A **41**, 49 (1990).

[25] D. C. Cartwright, S. Trajmar, W. Williams, and D. L. Huestis, Phys. Rev. Lett. **27**, 704 (1971).